2011-12-05

Nanozeolites Doped Photopolymer Layers with Reduced Shrinkage

Mohesh Moothanchery
Dublin Insitute of Technology

Izabela Naydenova
Technological University of Dublin, izabela.naydenova@tudublin.ie

Svetlana Mintova
ENSICAEN - Université de Caen – CNRS

See next page for additional authors

Recommended Citation

Moothanchery, M. (2011) Nanozeolites Doped Photopolymer Layers with Reduced Shrinkage. *Optics Express, Vol. 19, Iss. 25, pp. 25786-25791. doi:10.1364/OE.19.025786*

Nanozeolites doped photopolymer layers with reduced shrinkage

Mohesh Moothanchery,[1,3] Izabela Naydenova,[1,4] Svetlana Mintova,[2] and Vincent Toal[1]

[1]*Centre for Industrial & Engineering Optics, School of Physics, Dublin Institute of Technology Kevin Street, Dublin 8, Ireland*

[2]*Laboratoire Catalyse & Spectrochimie (LCS), ENSICAEN—Université de Caen—CNRS 6, boulevard du Maréchal Juin 14050, Caen Cedex, France*

[3]*mohesh.moothanchery@mydit.ie*

[4]*izabela.naydenova@dit.ie*

Abstract: An acrylamide based photopolymer doped with pure silica MFI-type zeolite (silicalite-1) nanoparticles has been characterized for holographic recording purposes. The concentrations of the silicalite-1 nanoparticles in the photopolymer layers were 1, 2.5, 5 and 7.5 wt. %. The inclusion of silicalite-1 nanoparticle in the photopolymer has resulted in an increase of the diffraction efficiency by up to 40%, and decrease of the shrinkage from 1.32% to 0.57%. The best results were obtained in layers doped with 5 wt. % silicalite-1 nanoparticles.

OCIS codes: (090.0090) Holography; (160.5470) Polymers; (090.7330) Volume gratings; (160.5335) Photosensitive materials; (160.4670) Optical materials.

References and links

1. J. Biles, "Holographic color filters for LCDs," SID Int. Symp. Dig. Technical Papers **25**, 403–406 (1994).
2. A. Pu and D. Psaltis, "High-density recording in photopolymer-based holographic three-dimensional disks," Appl. Opt. **35**(14), 2389–2398 (1996).
3. U.-S. Rhee, H. J. Caulfield, J. Shamir, C. S. Vikram, and M. M. Mirsalehi, "Characteristics of the DuPont photopolymer for angularly multiplexed page-oriented holographic memories," Opt. Eng. **32**(8), 1839–1847 (1993).
4. I. Naydenova, H. Sherif, S. Mintova, S. Martin, and V. Toal, "Holographic recording in nanoparticle doped photopolymer," Proc. SPIE **6252**, 625206 (2006).
5. P. Hemmer, S. Shahriar, J. Ludman, and H. J. Caulfield, "Holographic optical memories," in *Holography for the New Millennium,* J. Ludman, H. J. Caulfield, and J. Riccobono, eds. (Springer, 2002), pp. 179–189.
6. D. H. Close, A. D. Jacobson, J. D. Margerum, R. G. Brault, and F. J. McClung, "Hologram recording on photopolymer materials," Appl. Phys. Lett. **14**(5), 159–160 (1969).
7. K. Matyjaszewski and T. P. Davis, *Handbook of Radical Polymerization* (Wiley, 2002).
8. S.-J. Luo, G.-D. Liu, Q.-S. He, M.-X. Wu, G.-F. Jin, M.-Q. Shi, T. Wang, and F.-P. Wu, "Holographic grating formation in dry photopolymer film with shrinkage," Chin. Phys. **13**(9), 1428–1431 (2004).
9. O. Sakhno, L. Goldenberg, J. Stumpe, and T. Smirnova, "Surface modified ZrO_2 and TiO_2 nanoparticles embedded in organic photopolymers for highly effective and UV-stable volume holograms," Nanotechnology **18**(10), 105704 (2007).
10. R. A. Vaia, C. L. Dennis, L. V. Natarajan, V. P. Tondiglia, D. W. Tomlin, and T. J. Bunning, "One-step, micrometer-scale organization of nano- and mesoparticles using holographic photopolymerization, A generic technique," Adv. Mater. (Deerfield Beach Fla.) **13**(20), 1570 (2001).
11. I. Naydenova and V. Toal, "Nanoparticle doped photopolymers for holographic applications" in *Ordered porous Solids*, V. Valtchev, S. Mintova, and M. Tsapatsis, eds. (Elsevier, 2008)
12. N. Suzuki, Y. Tomita, and T. Kojima, "Holographic recording in TiO_2 nanoparticle-dispersed methacrylate photopolymer layers," Appl. Phys. Lett. **81**(22), 4121–4123 (2002).
13. C. Sánchez, M. J. Escuti, C. van Heesch, C. W. M. Bastiaansen, D. J. Broer, J. Loos, and R. Nussbaumer, "TiO_2 nanoparticle-photopolymer holographic recording," Adv. Funct. Mater. **15**(10), 1623–1629 (2005).
14. S. Martin, C. A. Feely, and V. Toal, "Holographic recording characteristics of an acrylamide-based photopolymer," Appl. Opt. **36**(23), 5757–5768 (1997).
15. I. Naydenova, H. Sherif, S. Mintova, S. Martin, and V. Toal, "Holographic recording in nanoparticle-doped photopolymer," Proc. SPIE **6252**, 625206 (2006).
16. T. Babeva, R. Todorov, S. Mintova, T. Yovcheva, I. Naydenova, and V. Toal, "Optical properties of silica MFI doped acrylamide-based photopolymer," J. Opt. A, Pure Appl. Opt. **11**(2), 024015 (2009).
17. H. Kogelnik, "Coupled wave theory for thick hologram gratings," Bell Syst. Tech. J. **48**(9), 2909 (1969).

#149873 - $15.00 USD Received 24 Jun 2011; revised 6 Oct 2011; accepted 6 Oct 2011; published 2 Dec 2011

18. H. Sherif, I. Naydenova, S. Martin, C. McGinn, and V. Toal, "Characterization of an acrylamide-based photopolymer for data storage utilizing holographic angular multiplexing," J. Opt. A, Pure Appl. Opt. **7**(5), 255–260 (2005).
19. J. T. Gallo and C. M. Verber, "Model for the effects of material shrinkage on volume holograms," Appl. Opt. **33**(29), 6797–6804 (1994).
20. A. Beléndez, I. Pascual, and A. Fimia, "Model for analyzing the effects of processing on recording material in thick holograms," J. Opt. Soc. Am. A **9**(7), 1214–1223 (1992).
21. I. Naydenova, E. Leite, T. Babeva, N. Pandey, T. Baron, T. Yovcheva, S. Sainov, S. Martin, S. Mintova, and V. Toal, "Optical properties of photopolymerizable nanocomposites containing nanosized molecular sieves," J. Opt. **13**(4), 044019 (2011).
22. M. Moothanchery, I. Naydenova, and V. Toal, "Study of the shrinkage caused by holographic grating formation in acrylamide based photopolymer film," Opt. Express **19**(14), 13395–13404 (2011).

1. Introduction

An ideal recording material for most holographic applications should have high spatial frequency response, high diffraction efficiency, low scattering and high sensitivity. For commercial purposes the material should be recyclable, have long shelf life and cheap. Photopolymers are one type of material under investigation for holographic applications including LCD displays [1] data storage [2–4] and optical elements [5] because of their easy processing, high light sensitivity, relatively high refractive index contrast and reasonable cost. In 1969, Close et al. [6] used photopolymer as a recording material for the first time. It consisted of a monomer, a photosensitive dye and an initiator. Dry photopolymers also contain a polymeric binder.

The photopolymer system consists of a dye sensitizer sensitive to the chosen recording wavelength, an electron donor in combination with sensitizers to generate free radicals to polymerize the monomer. In formulations with improved stability a second monomer is added acting as a cross linker. In dry photopolymer layers an inert background polymer acts as a binder and helps in forming the photosensitive layers. The polymerization process involves three steps, initiation, propagation and termination [7].

One of the main challenges in the use of photopolymers in holographic applications is the rotation of Bragg angle due to change in volume during recording [8]. Large refractive index modulation is rather difficult to achieve for pure polymer materials [9]. Bunning et al. [10] pioneered the idea of introducing inorganic nanoparticles which have substantially higher (or lower) refractive index than the photopolymer and act as a movable non-reactive component. Nanoparticles are known as non-reactive components with low scattering, high stability in water suspensions and with a broad range of refractive index [11]. The use of nanoparticles for photopolymer doping was further developed by other groups [10,12,13]. It was also demonstrated that the incorporation of nanoparticles helped to prevent change in the photopolymer volume [12].

The material reported here is an acrylamide based photopolymer developed at the Centre for Industrial and Engineering Optics [14]. Holographic characteristics such as diffraction efficiency and angular selectivity profile of the layers are studied in detail. Microporous silicate-1 nanoparticles with MFI structure and lower refractive index than the host photopolymer were used in our experiments. The microporous nanoparticles can introduce relatively low scattering, higher diffraction efficiency and lower shrinkage [15]. The refractive index of layers doped with pure silicalite-1 nanoparticles was characterized and reported previously [16]. After holographic recording the Bragg selectivity curves of slanted holographic gratings were obtained and analyzed. The curves were fitted using Kogelnik's coupled wave theory as explained in [17,18]. Assuming that the main volume change is associated with out-of-plane shrinkage, one can write the expression for the fractional change Δd in grating thickness d knowing the initial, ϕ_0, and the final ϕ_1 slant angles of the grating [19,20]. Hence the shrinkage is obtained as

$$\frac{\Delta d}{d} = \frac{\tan\phi_1}{\tan\phi_0} - 1 \tag{1}$$

#149873 - $15.00 USD Received 24 Jun 2011; revised 6 Oct 2011; accepted 6 Oct 2011; published 2 Dec 2011

2. Experimental procedures

2.1 Sample preparation

The photopolymer solution was prepared as described in [11]. To 1 ml of photopolymer solution silicalite-1 nanoparticles were added as colloidal aqueous suspensions in volumes of 0.18, 0.46, 0.94 and 1.44 ml containing 1.5 wt.% of nanoparticles. More water was added to equalize the solid substance concentrations in all stock solutions and to obtain the same thickness of the final nanocomposite layers. Finally, 1.1 ml of the suspension was spread on a 25 mm x 120 mm glass plate, and allowed to dry for 24 h. After drying, the samples were 40 ± 3 μm thick. The final concentrations of zeolite nanoparticles were 1, 2.5, 5 and 7.5 wt. %.

2.2 Holographic recording

The setup for recording holographic gratings is shown in Fig. 1. The 532 nm beam from a frequency doubled Nd-YVO4 laser was spatially filtered, expanded and collimated to around 1 cm cross sectional diameter by a lens and split into two beams using a beamsplitter. The beams were made to overlap completely at the photopolymer sample at equal and opposite angles of incidence thus ensuring a constant beam ratio across the illuminated area. The sample was mounted on a high-precision computer-controlled rotational stage (Newport M-URM100ACC), the plate normal bisecting the interbeam angle to ensure that the recorded grating was unslanted. The angle of incidence was 30.85° so that the spatial frequency was 1000 lines/mm. After recording the unslanted gratings and obtaining the angular selectivity profiles, the profiles of gratings recorded with slant angles of −10°, −5°, + 5° and + 10° were measured. These angles were slightly different in layers doped with silicalite-1 nanoparticles since inclusion of nanoparticles in the photopolymer, changes the average refractive index of the doped layer [16]. These changes were taken into account in analyzing the data.

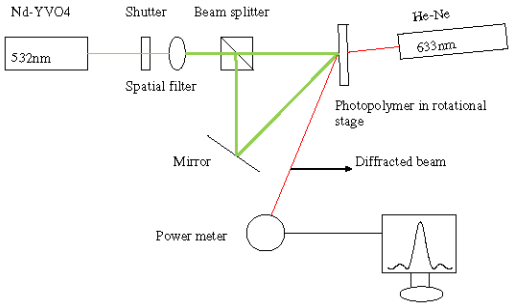

Fig. 1. Optical set-up for recording transmission phase holographic gratings.

The diffraction efficiencies of the gratings were monitored using a He-Ne beam, which was diffracted by the recorded grating but not absorbed by the photopolymer. The intensity of both the He-Ne laser incident on the grating and the diffracted intensity were measured using a power meter (Newport Optical Power Meter Model 1830-C). It was ensured that the He–Ne laser was incident at the Bragg angle for 633 nm light although there was a small deviation of from the exact Bragg angle (± 0.17°) in the position of maximum diffraction intensity outside the photopolymer layer for the unslanted gratings (this was taken into account in analysing the data). The angles of the He-Ne beam were 5.62°, 8.89°, 15.33° and 18.421°, respectively inside the undoped photopolymer layers.

3. Results and discussion

The dynamic light scattering (DLS) curve of silicalite-1 nanoparticles prior to mixing with the photopolymer is shown in Fig. 2. As can be seen the hydrodynamic diameter of the crystals is about 30 nm. The DLS curve is very narrow, confirming monomodal particle size distribution of the zeolite crystals. A TEM image of the crystalline silicalite-1 nanoparticles is shown in

#149873 - $15.00 USD Received 24 Jun 2011; revised 6 Oct 2011; accepted 6 Oct 2011; published 2 Dec 2011

the inset in Fig. 2. The crystalline nature of silicalite-1 particles is proven by the presence of crystalline fringes.

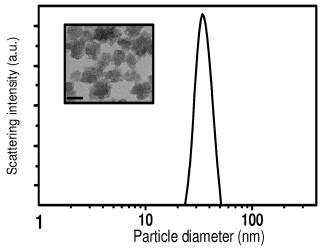

Fig. 2. Dynamic light scattering curve of silicalite-1 nanocrystals in water suspension prior mixing with the photopolymer; the inset shows a TEM picture of the crystalline particles (d = 30 nm).

The recording intensity and exposure time were 5 mW cm^{-2} and 16 seconds respectively. The growth curves of 10° slanted gratings recorded in layers with different concentrations of MFI nanocrystals are shown in Fig. 3(a). It is seen that the diffraction efficiency grows more rapidly with nanoparticle concentration up to 5% but slows again for 7.5% concentration probably because of increased scatter. To obtain the same ultimate diffraction efficiency in all layers would require longer exposures for layers with lower nanoparticle concentrations leading to correspondingly even greater shrinkage in them. Although these increases in shrinkage are expected to be smaller at later stage of recoding they should follow the same trend of lower shrinkage with increased doping concentration shown in Fig. 4b).

The corresponding angular selectivity curves are shown in Fig. 3(b). The shift of the Bragg curve decreased with increasing concentration of the zeolite nanocrystals. The same dependence of diffraction efficiency on nanoparticle concentration was observed for all other slant angles (+ 10°, −5°,-10°). Three different samples were measured at each slant angle. The difference in the initial position of the Bragg peak arises from the change in refractive index, as the nanoparticle doped layers have lower refractive index than the undoped layers. The shifts in the Bragg peaks for undoped (0%) and layers doped with 1%, 2.5%, 5%, 7.5% wt.% silicalite-1 concentrations are 0.094°, 0.063°, 0.058°, 0.051°, 0.049°, respectively.

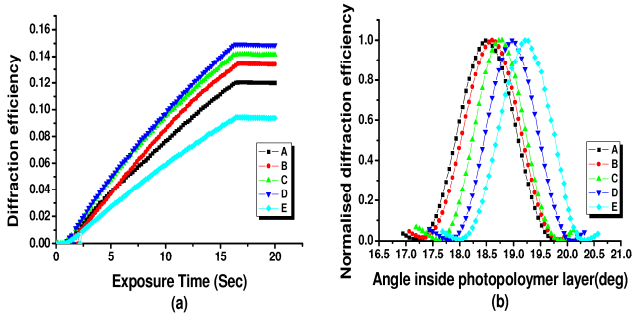

Fig. 3. (a) Diffraction efficiency growth and (b) angular selectivity curves for gratings with 10^0 slant angle recorded in A- undoped layer, and layers doped with B- 1%, C-2.5%, D-5%, E-7.5 wt. % silicalite-1 nanocrystals. (b) The corresponding shift in the peak position is A-0.094°, B-0.063°, C- 0.058°, D- 0.051°, E-0.049°.

The shrinkage was determined using Eq. (1) whose slope gives the shrinkage of the materials as a percentage. The shift in the Bragg peak versus slant angle for layers with different nanoparticle concentrations is shown in Fig. 4. As can be seen from Fig. 4(b), the shrinkage decreases with increasing concentration of nanoparticles. Lower shrinkage and higher diffraction efficiency with increased concentration of silicalite-1 have been obtained

#149873 - $15.00 USD Received 24 Jun 2011; revised 6 Oct 2011; accepted 6 Oct 2011; published 2 Dec 2011

for concentrations up to 5 wt.%. Increasing the concentration of nanoparticles to 7.5 wt.% decreases the shrinkage but increases the scatter and hence reduces the diffraction efficiency.

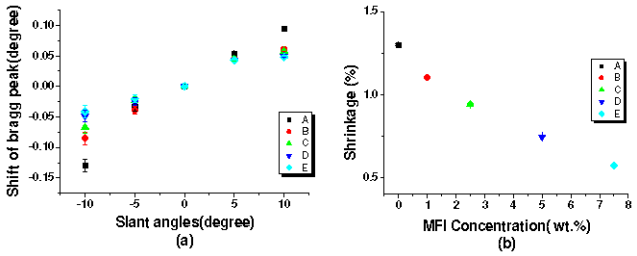

Fig. 4. (a) Bragg peak shift with respect to the initial slant angles for gratings recorded at A-0 wt.%; B- 1 wt.%, C- 2.5 wt.%, D-5 wt.%, E-7.5 wt. %. nanoparticles; (b) Dependence of shrinkage on concentration of the nanoparticles.

The observed increase in the diffraction efficiency in photopolymer doped with zeolite nanoparticles (Fig. 3a) is due to counter-diffusion processes during the holographic recording whereby monomers diffuse into bright regions as a result of a change in concentration gradient as polymerisation proceeds and the nanoparticles migrate from bright to dark regions during the recording. We can attribute the increase in diffraction efficiency to the increased refractive index modulation caused by nanoparticle redistribution [21].

We have also made recordings with 2.5 wt.% silicalite-1 nanoparticles in layers with different thicknesses. Gratings with slant angle of 5° were recorded in layers of thickness 45 μm, 85 μm and 125 μm at a recording intensity of 10 mWcm^{-2} and exposure time of 8s. Figure 5(a) shows the diffraction efficiency growth curves and Fig. 5(b) shows the corresponding Bragg curves. Higher diffraction efficiency was measured in the thicker layers but the percentage shrinkage was the same for all thicknesses. The percentage shrinkage was 0.79, 0.78, 0.8% for layers with thickness of 45, 85 and 125 μm, respectively. The absolute shrinkages, shown in Fig. 6(b), were 0.35 μm, 0.66 μm and 1 μm .

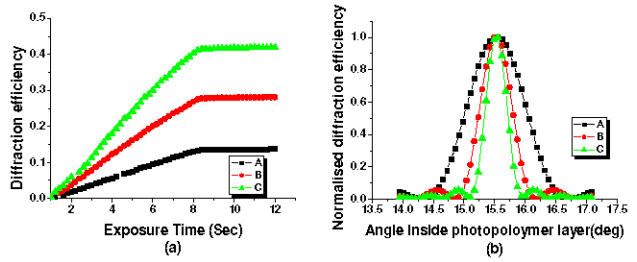

Fig. 5. (a) Diffraction efficiency growth and (b) angular selectivity curves for gratings with 5° slant angle recorded in layers having thickness of: A- 45 μm, B- 85 μm, C- 125 μm. The corresponding position of the Bragg peak in (b) is A –16.114°, B-16.111°, and C- 16.116°

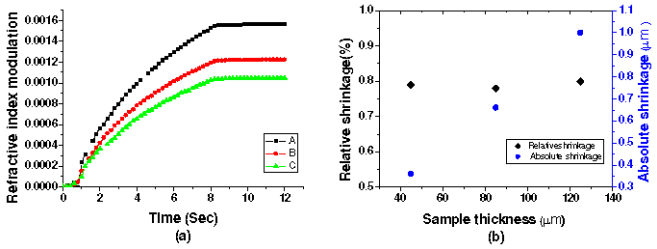

Fig. 6. (a) Dependence of refractive index modulation on exposure time and (b)shrinkage of layers with thickness of A-45µm, B-85µm, and C-125µm.

#149873 - $15.00 USD Received 24 Jun 2011; revised 6 Oct 2011; accepted 6 Oct 2011; published 2 Dec 2011

The dependence of the percentage shrinkage of the nanoparticle doped layers on their thickness differs from that observed previously in undoped layers [22], in which the percentage shrinkage decreased by a factor of three as layer thickness was increased from 30 to 120 μm. The refractive index modulation was calculated from the diffraction efficiency data and found to decrease with thickness (Fig. 6 (a)). A similar decrease in refractive index modulation with thickness was observed in undoped layers [22], but the effect was pronounced only above 60 μm layer thickness . This effect is probably due to attenuation of the recording beam intensity within the layer and, although the diffraction efficiency of gratings in thicker layers is higher, their average refractive index modulation is lower.

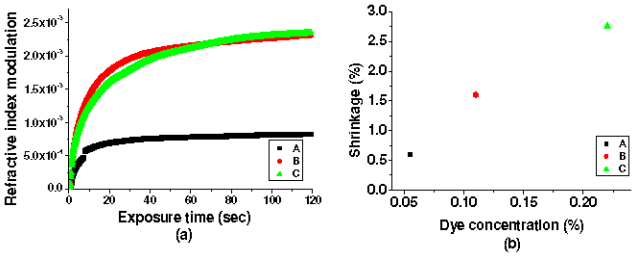

Fig. 7. Dependence of refractive index modulation on dye concentration (a) and percentage shrinkage dependence on dye concentrations (b) for dye concentrations A-0.055%, B-0.11%, C-0.22%

Results from experiments with layers with 2.5% MFI concentration and dye concentrations of 0.055%, 0.11% (the optimized concentration used in all previous experiments) and 0.22% are shown in Fig. 7. Exposure was at an intensity of 5mWcm^{-2} for 120 s. The refractive index modulation obtained (Fig. 7(a)) is significantly lower in layers with dye concentration of 0.055% and a dye concentration of 0.22% doesn't lead to any obvious improvement in the refractive index modulation. At the same time the shrinkage is seen to increase with dye concentration.

4. Conclusions

Transmission diffraction gratings of spatial frequency 1000 l/mm were recorded at constant exposure in acrylamide- based photopolymer layers of thickness 40 ± 3μm without and with zeolite nanoparticles in different concentrations. The Bragg curves and Kogelnik's coupled wave theory were used to fit the angular selectivity curves of the gratings. The grating thickness, and initial and final slant angles obtained from the Bragg curves were used to calculate the shrinkage of the layers. Higher shrinkage is measured for recording in undoped photopolymer and the shrinkage is reduced by up to one half with increasing concentration of zeolite nanoparticles. Recordings were also made in layers of different thicknesses doped with 2.5 wt.% nanopaticles, and no change in the shrinkage was measured in all cases.

The effects of doping of photopolymer layers with different microporous nanoparticles with various shapes and structures will be studied in order to clarify the mechanism of suppression of the photopolymer shrinkage.

Acknowledgments

MH is supported by a scholarship provided by the Technological Sector Research: Strand I-Post-Graduate R&D Skills Programme. The authors would like to acknowledge the School of Physics and FOCAS, DIT for technical support. The financial support of the SARA Programme, DIT is also acknowledged.

#149873 - $15.00 USD Received 24 Jun 2011; revised 6 Oct 2011; accepted 6 Oct 2011; published 2 Dec 2011